



Targeting CHAF1B Enhances IFN Activity against Myeloproliferative Neoplasm Cells

Diana Saleiro^{1,2}, Ewa M. Kosciuzuk^{1,2,3}, Mariafausta Fischietti^{1,2}, Ricardo E. Perez^{1,2}, G. Sohae Yang¹, Frank Eckerdt^{1,2}, Elspeth M. Beauchamp^{1,2,3}, Ye Hou⁴, Qixuan Wang⁴, Rona Singer Weinberg^{5,6}, Eleanor N. Fish⁷, Feng Yue^{1,4}, Ronald Hoffman^{6,8}, and Leonidas C. Platanias^{1,2,3}

ABSTRACT

Interferons (IFNs) are cytokines with potent antineoplastic and antiviral properties. IFN α has significant clinical activity in the treatment of myeloproliferative neoplasms (MPN), but the precise mechanisms by which it acts are not well understood. Here, we demonstrate that chromatin assembly factor I subunit B (CHAF1B), an Unc-51-like kinase 1 (ULK1)-interactive protein in the nuclear compartment of malignant cells, is overexpressed in patients with MPN. Remarkably, targeted silencing of *CHAF1B* enhances transcription of IFN α -stimulated genes and promotes IFN α -dependent

antineoplastic responses in primary MPN progenitor cells. Taken together, our findings indicate that CHAF1B is a promising newly identified therapeutic target in MPN and that CHAF1B inhibition in combination with IFN α therapy might offer a novel strategy for treating patients with MPN.

Significance: Our findings raise the potential for clinical development of drugs targeting CHAF1B to enhance IFN antitumor responses in the treatment of patients with MPN and should have important clinical translational implications for the treatment of MPN and possibly in other malignancies.

Introduction

Myeloproliferative neoplasms (MPN) are a group of hematologic malignancies characterized by aberrant myeloid cell proliferation and increased risk of transformation to acute myeloid leukemia (1, 2). There are three types of MPN: polycythemia vera (PV), essential thrombocythemia (ET), and primary myelofibrosis (PMF; refs. 3, 4). The somatic mutations that drive the development of MPN phenotypes occur in hematopoietic stem cells, the most common

being the substitution of a valine for a phenylalanine at the 617 position in the Janus kinase 2 gene (*JAK2*^{V617F}), an intracellular tyrosine kinase, which is activated downstream of the interaction between hematopoietic growth factors and their receptor (4–6). In addition, somatic mutations in *CALR* (calreticulin), *MPL* (MPL proto-oncogene, thrombopoietin receptor), and *TET2* (Tet methylcytosine dioxygenase 2) genes are also detected in patients with MPN (4).

Interferon-alpha (IFN α) is currently one of the drugs considered the standard of care for patients with PV and ET (7–10). Type I IFNs bind to specific cell-surface IFN receptors activating distinct signaling pathways that mediate the transcription and translation of IFN-stimulated genes (ISG), which ultimately account for their unique IFN biological effects (11–14). Although there have been substantial advances in our understanding of the IFN signaling, the connection and specificity of signaling events that correlate with clinical responses in MPN remains to be defined.

We have previously shown that Unc-51-like kinase 1 (ULK1) plays a central and essential role in the generation of IFN responses in PV (15, 16). In the current study, we identify chromatin assembly factor 1 subunit B (CHAF1B) as a novel negative regulator of IFN α -inducible ULK1-driven signaling pathways in MPN cells that may control IFN α -mediated anti-MPN responses. We demonstrate that CHAF1B, a protein component of the chromatin assembly factor 1 complex (CAF-1; ref. 17), is overexpressed in the peripheral blood (PB) of patients with MPN and interacts with ULK1 in the nuclear compartment. Disruption of *CHAF1B* expression strongly enhances the effects of IFN α on MPN cells. Our findings raise the possibility of clinical development of CHAF1B inhibitors to

¹Robert H. Lurie Comprehensive Cancer Center of Northwestern University, Chicago, Illinois. ²Division of Hematology-Oncology, Department of Medicine, Feinberg School of Medicine, Northwestern University, Chicago, Illinois. ³Department of Medicine, Jesse Brown Veterans Affairs Medical Center, Chicago, Illinois. ⁴Department of Biochemistry and Molecular Genetics, Feinberg School of Medicine Northwestern University, Chicago, Illinois. ⁵The New York Blood Center, New York, New York. ⁶Myeloproliferative Neoplasms Research Consortium, New York, New York. ⁷Toronto General Hospital Research Institute, University Health Network & Department of Immunology, University of Toronto, Toronto, Ontario, Canada. ⁸Tisch Cancer Institute, Icahn School of Medicine at Mount Sinai, New York, New York.

D. Saleiro and E.M. Kosciuzuk contributed as co-first authors to this article.

Corresponding Author: Leonidas C. Platanias, Robert H. Lurie Comprehensive Cancer Center of Northwestern University, 303 East Superior Street, Lurie 3-125, Chicago, IL 60611-3008. Phone: 312-503-4755; E-mail: l-platanias@northwestern.edu

doi: 10.1158/2767-9764.CRC-23-0010

This open access article is distributed under the Creative Commons Attribution 4.0 International (CC BY 4.0) license.

© 2023 The Authors; Published by the American Association for Cancer Research

enhance IFN α -driven antitumor responses in MPN and possibly additional IFN-responsive malignancies.

Materials and Methods

Cells, Cell Culture, and Reagents

HEL cells (#TIB-180; ATCC; RRID:CVCL_2481) were cultured in RPMI1640 medium (Gibco) supplemented with 10% FBS and antibiotics. SET-2 cells (#ACC 608; DSMZ; RRID:CVCL_2187) were cultured in RPMI1640 medium (Gibco) supplemented with 20% FBS and antibiotics. All cell lines were frozen at low passage in liquid nitrogen and were kept in culture for no longer than 15 passages. All cells were routinely tested for *Mycoplasma* contamination using a MycoAlert PLUS *Mycoplasma* detection kit, following the manufacturer's instructions (Lonza). Cell lines were authenticated by short tandem repeat analyses and matched to the ATCC or DSMZ database every 6 months to 1 year.

PB from PV patients was collected after obtaining written informed consent approved by the Institutional Review Board of Northwestern University (Chicago, IL) and PB mononuclear cells (MC) were isolated following Histopaque density gradient separation (Sigma). PBMcs or bone marrow (BM) MCs from PV patients were also obtained from the New York Blood Center bank. These samples were collected from patients with PV who participated in the Myeloproliferative Disorders Research Consortium (MPD-RC-III) study, after obtaining patients' written informed consent and approved by the respective Institutional Review Boards of Institutions participating in the MPN Research Consortium. The MPD-RC-III study was an investigator-initiated, international, multicenter, phase II trial evaluating the ability of pegylated-rIFN- α 2a therapy to induce complete and partial hematologic responses in patients with high-risk ET or PV who were either refractory or intolerant to hydroxyurea (clinical trial #NCT01259817). PBMcs or BMMcs were collected at baseline, prior to IFN treatment. The criteria for enrollment of patients and a detailed description of participants enrolled in clinical trial #NCT01259817 have been described previously (18).

ON-TARGETplus non-targeting control pool siRNAs (#D-001810-10-05) and human *CHAF1B* SMARTPool siRNAs (#L-019937-00-0005) were purchased from Horizon Discovery (Dharmacon). Control and *ULK1* targeting siRNAs were obtained from Santa Cruz Biotechnology (control siRNA-H #sc-44236 and human *ULK1* siRNA #sc-44182). Anti-*CHAF1B* antibody (WB - 1:1,000, ChIP: 2 μ g/IP; #27633-1-AP, RRID:AB_2880933) was from Proteintech. Anti-*ULK1* (WB - 1:1,000, co-IP - 2.1 μ g/mg protein lysate; #8054, RRID:AB_11178668) and anti-lamin A/C (WB - 1:1,000, #2032, RRID:AB_2136278) antibodies were from Cell Signaling Technology and anti- α -tubulin antibody (WB - 1:1,000, #sc-5286, RRID:AB_628411) was from Santa Cruz Biotechnology. Anti-GAPDH antibody (WB - 1:20,000, #MAB374, RRID:AB_2107445) was from EMD Millipore. The *ULK1* inhibitor SBI-0206965 (SBI) was purchased from Cayman Chemical (#18477).

Nano-LC/MS-MS Analysis

To identify new binding partners for endogenous *ULK1*, HEL cells were either left untreated or were treated with recombinant human interferon alfacon-1 (IFN α ; 5×10^3 IU/mL) for 4 hours, then lysed to isolate cytoplasmic and nuclear proteins using the NE-PER Nuclear and Cytoplasmic Extraction Reagents (Thermo Fisher Scientific, #78833) according to the manufacturer's protocol. Three milligrams of cytoplasmic and nuclear cell protein lysates, respectively

from untreated and IFN α -treated samples were used for immunoprecipitation (IP) of endogenous *ULK1* complexes using *ULK1* (D8H5) rabbit mAb (2.1 μ g/mg protein; Cell Signaling Technology, #8054, RRID:AB_11178668). As control, the same procedure was followed for IFN α -treated lysates but using rabbit (DA1E) mAb IgG XP isotype control (Cell Signaling Technology, #3900, RRID:AB_1550038) instead of the *ULK1* antibody. After incubating the samples with antibody overnight with rotation at 4°C, these were incubated with protein G sepharose 4 Fast Flow beads (GE Healthcare) for 1 hour with rotation at 4°C, then washed two times with NP-40 buffer [20 mmol/L Hepes (pH 7.4), 180 mmol/L KCl, and 0.2 mmol/L Ethyleneglycol-bis(β -aminoethyl)-N,N,N',N'-tetraacetic Acid (EGTA), 0.1% NP-40] and one time with washing buffer [20 mmol/L Hepes (pH 7.4), 180 mmol/L KCl, and 0.2 mmol/L EGTA]. Protein-*ULK1* complexes were eluted from the beads by incubation with Lane Marker Reducing Sample Buffer (Pierce) at 95°C for 10 minutes, and proteomic analyses were performed by the Northwestern Proteomics Core Facility (Northwestern University, Chicago, IL), as in previous studies (16, 19).

Protein Function Enrichment Analysis

Protein lists identified in nano-liquid chromatography tandem mass spectrometry analysis (nLC/MS-MS), before and after IFN α treatment, in cytosolic and nuclear fractions were converted to gene lists that were submitted to the Metascape database (<http://metascape.org>; RRID:SCR_016620) for pathway and process enrichment analysis (20), as in our previous studies (19).

co-IP and Immunoblotting

HEL and SET-2 cells were either left untreated or were treated with IFN α (5×10^3 IU/mL) for either 10 minutes or 4 hours, as indicated. Cells were lysed to isolate cytoplasmic and nuclear proteins using the NE-PER Nuclear and Cytoplasmic Extraction Reagents, according to the manufacturer's protocol. A total of 700 μ g of protein lysates from cytoplasmic and nuclear fractions were used for IP of endogenous protein-*ULK1* complexes and were incubated overnight at 4°C with rotation with *ULK1* (D8H5) rabbit mAb (2.1 μ g/mg protein; Cell Signaling Technology, #8054, RRID:AB_11178668), followed by incubation for 1 hour at 4°C with rotation with protein G Sepharose 4 Fast Flow beads (GE Healthcare). As control, the same procedure was followed, using nonimmune rabbit IgG XP Isotype control antibody (DA1E; Cell Signaling Technology, #3900, RRID:AB_1550038) instead of anti-*ULK1* antibody. After the incubation, the beads were washed three times with NP-40 buffer [20 mmol/L HEPES (pH 7.4), 180 mmol/L KCl, 0.2 mmol/L EGTA, and 0.1% NP-40]. Protein-*ULK1* complexes were eluted from the beads by incubation with Lane Marker Reducing Sample Buffer (Pierce) at 95°C for 10 minutes. Eluates were resolved by SDS-PAGE and transferred to an Immobilon-P polyvinylidene difluoride (PVDF) membrane (Millipore). For immunoblotting analyses, the membranes were then probed with primary antibodies, followed by horseradish peroxidase-conjugated secondary antibodies, and antibody binding was detected by enhanced chemiluminescence using Amersham Biosciences ECL Prime Western blotting detection reagent (GE Healthcare Life Sciences), as in our previous studies (16, 19).

CHAF1B Expression in Patients with MPN

\log_2 of transcript levels of *CHAF1B* in neutrophils from patients with MPN with PV, ET, and PMF compared with healthy individuals was calculated using GSE54646 dataset (21) accessible through NCBI Gene Expression Omnibus (GEO; RRID:SCR_005012) database (22). In addition, using the mutational status information available for the same cohort of patients with MPN, we

compared \log_2 of *CHAFIB* levels in patients carrying wild-type versus mutant *JAK2*, *CALR*, *TET2*, and *MPL* genes.

qRT-PCR

HEL and SET-2 cells were transfected with either control siRNA or siRNAs targeting *CHAFIB* using Amaxa Biosystems Nucleofector Kit V and program X-005 for HEL cells and X-013 for SET-2 cells (Lonza) per the manufacturer's instructions. After 48 hours, transfected cells were either left untreated or were treated with IFN α (5×10^3 IU/mL) for 6 hours. RNA was isolated using the RNeasy Mini Kit (Qiagen) per the manufacturer's instructions. A total of 2 μ g of total cellular mRNA was reverse transcribed into cDNA using the OmniScript RT kit (Qiagen) and oligo(dT)12–18 primers (Life Technologies). qRT-PCR was carried out using the Bio-Rad CFX96 Real-Time System machine (Bio-Rad) using commercially available FAM-labeled probes and primers (Thermo Fisher Scientific) to determine the expression of human *CHAFIB* (Hs01123302_m1), *ISG15* (Hs01921425_s1), *MXI1* (Hs00895608_m1), *IFIT1* (Hs00356631_g1), and *IRF7* (Hs01014809_g1). Human *GAPDH* (Hs02758991_g1) was used for normalization. Relative quantitation of mRNA levels was calculated using the $\Delta\Delta$ Ct method and plotted as fold increase compared with control siRNA-transfected untreated cells.

Chromatin Immunoprecipitation Assay

Chromatin immunoprecipitation (ChIP) assays were performed as reported previously (23) using untreated versus IFN α -treated HEL cells, untreated versus IFN α -treated control siRNA and *ULK1* siRNA-transfected HEL cells, and vehicle (DMSO), SBI-0206965 (10 μ mol/L) and/or IFN α -treated HEL cells, as indicated in the respective figure legends, and using the SimpleChIP Enzymatic Chromatin IP Kit with Magnetic Beads (#9003, Cell Signaling Technology) per manufacturer's instructions. HEL cells were transfected with either control siRNA or siRNAs targeting *ULK1* using Amaxa Biosystems Nucleofector Kit V and program X-005 (Lonza) per the manufacturer's instructions one day prior to IFN α treatment. Anti-CHAFIB antibody (Proteintech, #27633-1-AP, RRID:AB_2880933) was used for IP of CHAFIB, and normal rabbit IgG (Cell Signaling Technology, #2729, RRID:AB_1031062) was used as negative control. qRT-PCR was performed on purified immunoprecipitated DNA for the *ISG15* and *IFIT1* promoter binding sites using SsoAdvanced Universal SYBR Green supermix (Bio-Rad) following manufacturer's guidelines with the following primers: *ISG15* FWD 5'-CCA CTT TTG CTT TTC CCT GTC-3', *ISG15* REV 5'-AGT TTC GGT TTC CCT TTC CC-3' and *IFIT1* FWD 5'-GGT TGC AGG TCT GCA GTT TAT CTG T-3' and *IFIT1* REV 5'-AGC TGT GGG TGT GTC CTT GC-3'. All qRT-PCR signals were normalized to the input DNA.

Hematopoietic Cell Progenitor Assays

In the experiments to assess the role of CHAFIB in the inhibitory effects of IFN α -mediated anticolonogenic effects, HEL and SET-2 cells were transfected with either control siRNA or siRNAs targeting *CHAFIB* using Amaxa Biosystems Nucleofector Kit V and program X-005 for HEL cells and X-013 for SET-2 cells (Lonza) per the manufacturer's instructions. Twenty-four hours later, control siRNA or *CHAFIB* siRNA-transfected cells were plated in MethoCult H4534 Classic medium (#04534, StemCell Technologies) and were either left untreated or were treated with IFN α (100 IU/mL for HEL and 50 IU/mL for SET-2). Leukemic colony-forming units (CFU-L) formation was assessed as in our previous studies (15, 16, 24). In addition, primary P BMCs or BMMCs from patients with PV were transfected with either control siRNA or *CHAFIB* siRNAs using TransIT-TKO Transfection Reagent (Mirus) and were

either left untreated or were treated with IFN α (1,000 IU/mL). Human erythroid progenitor cells [burst-forming unit erythroid (BFU-E)] were assayed in MethoCult H4434 Classic medium (#04434, StemCell Technologies), as described in our previous studies (15, 16). Data are expressed as the percentage of colony formation over untreated control siRNA-transfected cells.

Statistical Analyses

All statistical analyses were performed using GraphPad Prism 8.0 (RRID:SCR_002798). Statistical tests used are described in each figure legend. *P* values less than 0.05 were considered statistically significant.

Data Availability

The original data that support the findings of this study are available from the corresponding author upon reasonable request. The mass spectrometry proteomics data generated in this study have been deposited to the ProteomeXchange Consortium (RRID:SCR_004055) via the PRIDE partner (25) repository with the dataset identifier PXD037376.

Results

Proteomic Screening Identifies CHAFIB as a Novel Binding Partner of ULK1

In previous studies, we had identified ULK1 as a key regulator of IFN α -inducible antineoplastic responses in MPN (15, 16). In further studies, we sought to identify novel regulators of IFN α -ULK1-driven responses in *JAK2*^{V617F}-positive MPN-derived cells. As earlier reports have shown that ULK1 plays a role in both cytoplasmic and nuclear compartments (26, 27), we initiated these studies by performing co-IP of endogenous ULK1-protein complexes from cytoplasmic and nuclear fractions isolated from untreated and IFN α -treated *JAK2*^{V617F}-positive HEL cells, followed by nLC/MS-MS analysis. We observed that ULK1 potentially interacts in the cytosolic fraction with 16 proteins in untreated cells, 63 proteins under both untreated and IFN α -treated (4 hours) conditions and with 14 proteins after 4 hours of IFN α treatment (Fig. 1A, cytosolic fraction). In the nuclear fraction, ULK1 was found to potentially bind 29 proteins under untreated conditions, 72 proteins under both untreated and IFN α -treated (4 hours) conditions and 41 proteins after 4 hours of IFN α treatment (Fig. 1A, nuclear fraction; ProteomeXchange Consortium dataset identifier: PXD037376). Moreover, overlap analysis of the 63 and 72 putative binding partners of ULK1 found under untreated and IFN α -treated conditions in the cytosolic and nuclear fractions, respectively, revealed eight proteins that could potentially interact with ULK1 in both compartments under these conditions (Fig. 1B, UT + IFN α). Gene ontology analyses were then performed for the 63 cytosolic and 72 nuclear putative ULK1-interacting proteins found under both untreated and IFN α -treated conditions. We found that ULK1 potentially binds proteins involved in several biological processes, including viral processes, mTOR signaling, and cell cycle (Fig. 1C; Supplementary Fig. S1). Interestingly, ULK1 was found to potentially bind CHAFIB both in the cytosolic and nuclear compartments (Fig. 1A and B), a protein involved in regulation of DNA metabolic process and part of the chromatin assembly complex (Fig. 1C; Supplementary Fig. S1). Notably, CHAFIB has been shown to be essential for normal hematopoiesis, and its overexpression has been reported to contribute to leukemogenesis (28). We next validated the binding between ULK1 and CHAFIB in untreated and IFN α -treated *JAK2*^{V617F}-positive cells by co-IP followed by immunoblotting analyses. ULK1 specifically associated with CHAFIB

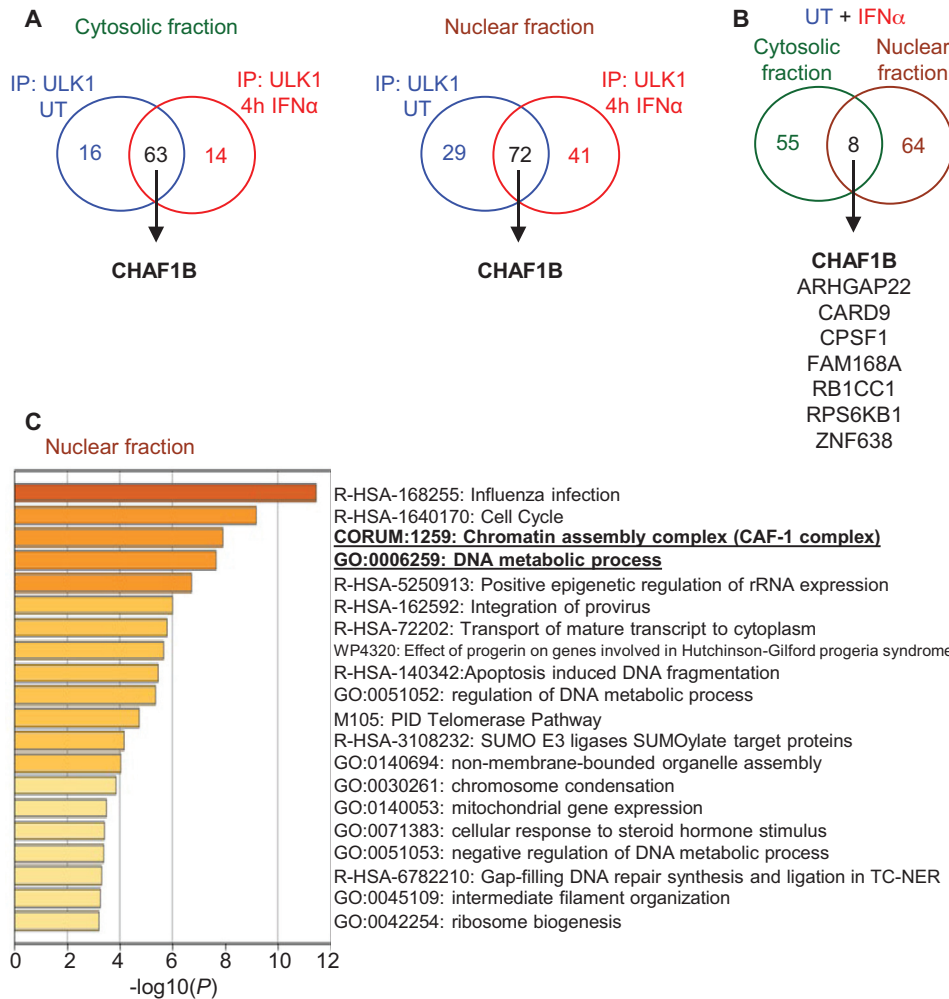


FIGURE 1 Mass spectrometry identification of cytosolic and nuclear putative binding partners of ULK1. **A** and **B**, Endogenous ULK1-protein complexes were immunoprecipitated (IP) using an anti-ULK1 antibody from cytosolic and nuclear fractions isolated from untreated (UT) or IFN α -treated [4 hours (4h)] HEL cells and analyzed by nLC/MS-MS. As negative control, IP with normal rabbit IgG was used instead of anti-ULK1 antibody and proteins bound to rabbit IgG were excluded from the analyses. **A**, Venn diagrams show the number of putative ULK1 binding partners identified only in untreated cells (blue), only in IFN α -treated cells (red), or both treated and untreated cells (black). CHAF1B was detected in both cell compartments by mass spectrometry. **B**, Venn diagram shows the overlap for the putative ULK1 binding partners identified under both untreated and IFN α -treated cells in the cytosolic and nuclear fractions. List of the putative ULK1 binding proteins found under these conditions on both cytosolic and nuclear compartments is shown. **C**, Gene ontology analyses of the 72 putative nuclear ULK1-interacting proteins identified under both untreated and IFN α -treated conditions are shown. Underlined and in bold are the biological events in which CHAF1B is involved.

in the nuclear compartment of both HEL and SET-2 cells (Fig. 2A and B). Importantly, using a previously published dataset (GEO accession: GSE54646; ref. 21), we found that the expression of *CHAF1B* is significantly upregulated in neutrophils isolated from patients with MPN with PV, ET, and PMF, when compared with neutrophils isolated from healthy donors (Fig. 2C). Interestingly, using the same dataset (GEO accession: GSE54646; ref. 21), when comparing the expression of *CHAF1B* in mutant versus wild-type cohorts for the *JAK2*, *CALR*, and *TET2* genes among patients with MPN (Fig. 2D–F), *CHAF1B* was found to be significantly higher in patients with MPN carrying a *CALR* mutation compared with patients carrying wild-type *CALR* (Fig. 2E). In this dataset (GEO accession: GSE54646), there was only information of 2 PMF patients carrying a *MPL* mutation, so no further analysis was performed for this gene.

CHAF1B Negatively Regulates IFN α -inducible Transcription of ISGs

As CHAF1B has been shown to compete with transcription factors at specific DNA-binding sites impairing transcription of myeloid differentiation genes in leukemic cells (28), we next sought to determine whether CHAF1B plays a role in IFN α -dependent transcription of ISGs in *JAK2*^{V617F}-positive cells. For this, we tested the effects of siRNA-mediated knockdown of *CHAF1B* on IFN α -induced transcription of ISGs in HEL and SET-2 cells using qRT-PCR analyses (Fig. 3A and B, left). Our results show that knockdown of *CHAF1B* increases IFN α -inducible mRNA expression of several ISGs (Fig. 3A and B). Moreover, through ChIP assays, CHAF1B was found to associate with the promoter regions of IFN-stimulated response element (ISRE) sites of *ISG15* and *IFIT1*

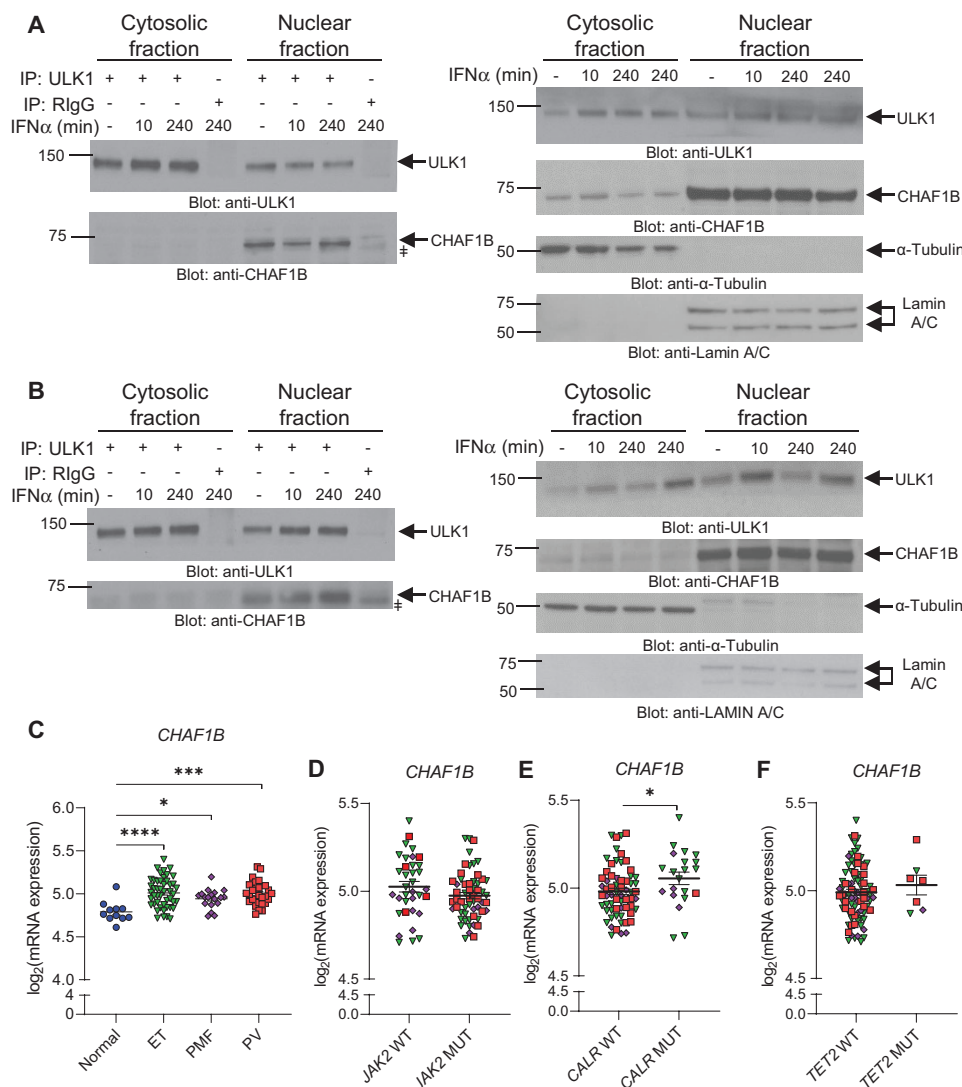


FIGURE 2 CHAF1B interacts with ULK1 in the nuclear compartment of *JAK2*^{V617F}-positive cells and is overexpressed in patients with MPN. **A** and **B**, Left, ULK1-protein complexes were co-IP using an anti-ULK1 antibody from cytosolic and nuclear protein fractions isolated from untreated or IFN α -treated (10 or 240 minutes) HEL (**A**) or SET-2 (**B**) cells and then resolved by SDS-PAGE. As control, cytosolic and nuclear lysates isolated from cells treated with IFN α for 240 minutes were incubated with normal rabbit IgG (RlgG) antibody. Interaction between ULK1 and CHAF1B was assessed by immunoblotting with anti-ULK1 and anti-CHAF1B antibodies. Note: †, unspecific band. **A** and **B**, Right, Equal amounts of cytosolic and nuclear protein lysates isolated from untreated and IFN α -treated HEL (**A**) and SET-2 (**B**) cells used for co-IPs were resolved by SDS-PAGE, transferred to PVDF membranes and then immunoblotted with antibodies against ULK1, CHAF1B, α -tubulin (cytosolic marker), and lamin A/C (nuclear marker), as indicated. **A** and **B**, Blots are representative of three independent experiments. **C**, Scatter dot plot of log₂ *CHAF1B* mRNA expression in neutrophils from healthy individuals (normal, $n = 11$) and patients with ET ($n = 47$), PMF ($n = 18$), and PV ($n = 28$). Data were extracted from NCBI GEO: GSE54646 study (21) and analyzed using GraphPad Prim 8. Shown are means \pm SEM. Statistical analysis was performed using one-way ANOVA followed by Dunnett multiple comparisons test to assess P values between patients with MPN and healthy individuals. *, $P < 0.05$; ***, $P < 0.001$; ****, $P < 0.0001$. Scatter dot plots of log₂ *CHAF1B* mRNA expression in neutrophils from patients with ET (green triangles), PMF (purple diamonds), and PV (red squares) carrying wild-type (WT) or mutant (MUT) *JAK2* (**D**), *CALR* (**E**), and *TET2* (**F**) genes (*JAK2* WT: ET $n = 20$, PMF $n = 10$, PV $n = 5$; *JAK2* MUT: ET $n = 26$, PMF $n = 8$, PV $n = 23$; *CALR* WT: ET $n = 27$, PMF $n = 11$, PV $n = 26$; *CALR* MUT: ET $n = 15$, PMF $n = 5$, PV $n = 1$; *TET2* WT: ET $n = 45$, PMF $n = 17$, PV $n = 24$; *TET2* MUT: ET $n = 2$, PMF $n = 1$, PV $n = 4$). Data were extracted from NCBI GEO: GSE54646 study (21) and analyzed using GraphPad Prim 8. Patients for which no information was available for the mutational status for the *JAK2*, *CALR*, or *TET2* genes were excluded from the analysis. Shown are means \pm SEM. Statistical analyses were performed using two-sample two-tailed t test: *, $P < 0.05$.

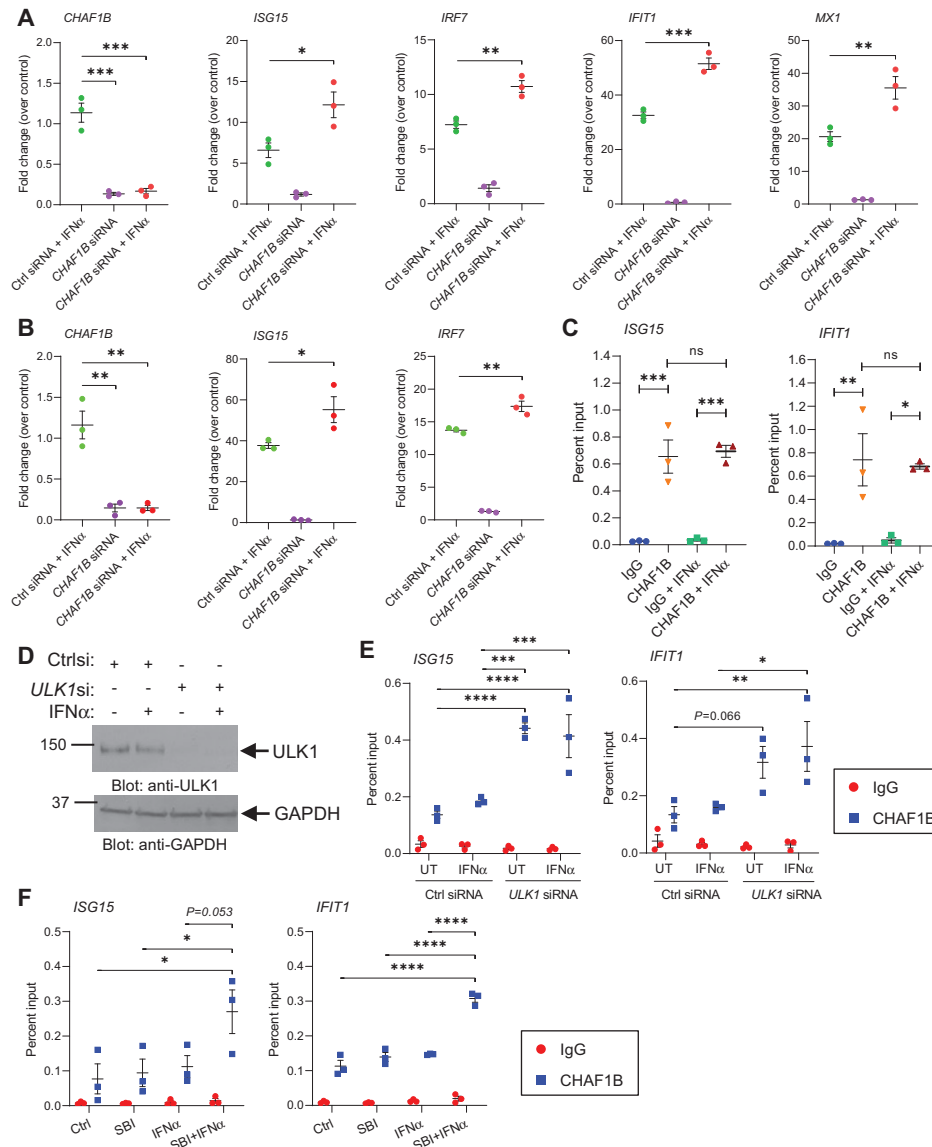


FIGURE 3 Gene-targeted inhibition of *CHAF1B* increases IFN α -inducible mRNA expression of ISGs in *JAK2*^{V617F}-positive leukemic cells. qRT-PCR analyses of the indicated genes in control (Ctrl) siRNA or *CHAF1B* siRNA-transfected *JAK2*^{V617F}-positive HEL (**A**) and SET-2 (**B**) cells, either left untreated or treated with IFN α for 6 hours. *GAPDH* mRNA expression was used for normalization. Data are expressed as fold change over control siRNA-transfected untreated cells (control) and represent means \pm SEM of three independent experiments for each cell line. Statistical analyses were performed using one-way ANOVA followed by Tukey multiple comparisons test. *, $P < 0.05$; **, $P < 0.01$; ***, $P < 0.001$. **C**, ChIP assay was performed in untreated and IFN α -treated (for 6 hours at 5,000 IU/mL) HEL cells at the *ISG15* promoter and the *IFIT1* promoter for *CHAF1B* binding using an anti-*CHAF1B* antibody. IgG antibody was used for each promoter region as negative control. Scatter dot plots show data as percent enrichment relative to input \pm SEM for three independent experiments. Statistical analyses were performed using one-way ANOVA followed by Tukey multiple comparisons test. ns, not significant; *, $P < 0.05$; **, $P < 0.01$; ***, $P < 0.001$. **D**, Immunoblot analysis of ULK1 expression in control siRNA (Ctrl si) and *ULK1* siRNA (*ULK1* si) transfected HEL cells either left untreated or treated with IFN α (for 6 hours at 5,000 IU/mL), as indicated. GAPDH levels were used as loading control. Blots are representative of three independent experiments used to perform ChIP assays shown in **E**. **E**, ChIP assay was performed in untreated (UT) and IFN α -treated control (Ctrl) siRNA- and *ULK1* siRNA-transfected HEL cells at the *ISG15* promoter and the *IFIT1* promoter for *CHAF1B* binding using an anti-*CHAF1B* antibody. **F**, HEL cells were pretreated for 1 hour with either DMSO (Ctrl) and IFN α groups) or SBI-0206965 (SBI; 10 μ mol/L; SBI and SBI+IFN α groups) followed by 6 hours of treatment with either DMSO (Ctrl), SBI (10 μ mol/L), IFN α (5,000 IU/mL) or SBI+IFN α , as indicated. ChIP assay was performed in HEL cells at the *ISG15* promoter and the *IFIT1* promoter for *CHAF1B* binding using an anti-*CHAF1B* antibody. **E** and **F**, IgG antibody was used for each promoter region as negative control. Scatter dot plots show data as percent enrichment relative to input \pm SEM for three independent experiments. Statistical analyses were performed using two-way ANOVA followed by Tukey multiple comparisons test: *, $P < 0.05$; **, $P < 0.01$; ***, $P < 0.001$; ****, $P < 0.0001$. Relevant statistical differences are shown for the binding of *CHAF1B* to *ISG15* and *IFIT1* promoter regions between experimental conditions.

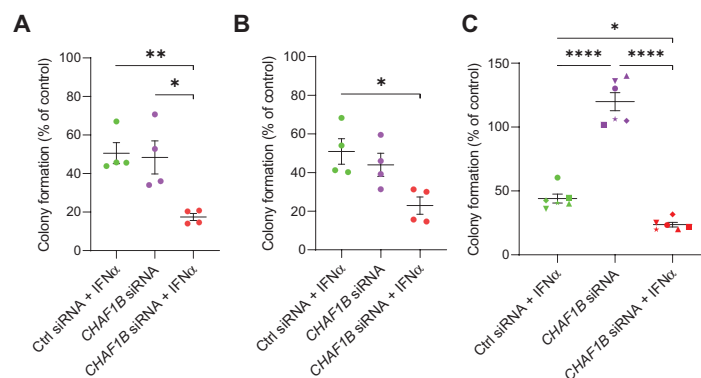


FIGURE 4 Inhibition of *CHAF1B* increases IFN α -induced anticolonogenic effects in MPN. HEL cells (**A**) and SET-2 cells (**B**) were transfected with either control (Ctrl) siRNA or *CHAF1B* siRNA, and leukemic CFU-L colony formation was assessed in clonogenic assays in the presence or absence of IFN α , as indicated. Data are expressed as percentage of colony formation over control siRNA-transfected untreated cells (control), and the scatter dot plots represent means \pm SEM of four independent experiments for each cell line. **C**, Clonogenic capability of primary malignant erythroid progenitors isolated from PV patients transfected with either control (Ctrl) siRNA or *CHAF1B* siRNA and either left untreated or treated with IFN α , as indicated. Data are expressed as percentage of colony formation over control siRNA-transfected untreated cells (control) and shown are means \pm SEM of six independent experiments using cells from six different patients with PV. Percentages for the same patient are represented by the same symbol and different patients have different symbols. **A–C**, Statistical analyses were performed using one-way ANOVA followed by Tukey multiple comparisons test. *, $P < 0.05$; **, $P < 0.01$; ****, $P < 0.0001$.

(Fig. 3C). Thus, elevated *CHAF1B* expression in MPN cells may prevent the binding of transcription factors to the promoter region of ISGs, thereby impairing IFN responses. Next, to assess whether interaction of ULK1 with *CHAF1B* in the nucleus affects *CHAF1B* binding to ISGs' promoter regions, we performed ChIP assays for *CHAF1B* using untreated and IFN α -treated control siRNA and *ULK1* siRNA-transfected HEL cells (Fig. 3D and E). Knockdown of *ULK1* was found to increase the binding of *CHAF1B* to ISRE sites on *ISG15* and *IFIT1* (Fig. 3E). In addition, drug-targeted inhibition of *ULK1* using SBI-0206965 (29) increased the binding of *CHAF1B* to the promoter region of *ISG15* and *IFIT1* when HEL cells were cotreated with IFN α (Fig. 3F). These results are consistent with our previous studies in which we show that *ULK1* is required for increased transcription of ISGs (15, 16) and suggest that *ULK1* prevents further binding of *CHAF1B* to ISGs' promoter regions, facilitating the binding of IFN-activated transcription factors.

CHAF1B Represses IFN α -dependent Antineoplastic Responses in MPN

Next, to determine whether inhibition of *CHAF1B* affects IFN α -dependent antineoplastic responses, we performed colony assays evaluating the effects of siRNA-mediated knockdown of *CHAF1B* in HEL and SET-2 cells. IFN α treatment decreased the growth of colonies in HEL and SET-2 cells transfected with control siRNA, and this suppression was greatly increased in cells in which *CHAF1B* was knocked down (Fig. 4A and B). In further studies, we demonstrated that knockdown of *CHAF1B* was found to enhance the IFN α -induced antineoplastic effects against primary PV patient-derived progenitor cells in clonogenic assays (Fig. 4C). Together, our data suggest that the high levels of *CHAF1B* in MPN cells suppress the antitumor effects of IFN α .

Discussion

Over the last decade, there have been substantial efforts to develop new therapeutic approaches for Philadelphia chromosome-negative myeloproliferative

neoplasms and to ameliorate the complications from the disease and to prevent evolution into acute leukemia (8, 30, 31). The clinical development of pegylated forms of IFN α have resulted in easier to use and better tolerated regimens, with substantial efficacy (7, 9, 10, 32). However, some patients respond poorly to IFN α therapy (7, 9, 10, 32), underscoring the need for new therapeutic approaches to enhance IFN sensitivity and optimize clinical responses.

In previous work, we demonstrated that the kinase *ULK1* is essential for the generation of IFN responses in MPN (15, 16). This prompted further studies to identify *ULK1*-interactive proteins that could be targeted therapeutically. Using mass spectrometry analysis screening, we identified *CHAF1B* as a novel interactor protein of *ULK1* in the nuclear compartment of *JAK2^{V617F}*-positive leukemic cells. *CHAF1B* is a component of the CAF-1 complex involved in the formation and loading of histone octamers during DNA replication (33, 34). Elevated CAF-1 correlates with a poor prognosis and decreased survival in numerous malignancies (35). In previous studies, we identified *ULK1* activity in the cytoplasmic compartment as required for IFN responses, independent of its autophagy-related role (15, 16, 36). As overexpression of *CHAF1B* is a driver of leukemogenesis by blocking the binding of transcription factors to DNA sequences of myeloid differentiation genes (28), we decided to further investigate its role on IFN α -driven responses in MPN. We found that *CHAF1B* is overexpressed in neutrophils of patients with MPN as compared with healthy individuals. Inhibition of *CHAF1B* expression enhanced transcription of ISGs and IFN α -induced anticolonogenic effects against *JAK2^{V617F}*-positive leukemic cells and primary PV patient cells. We show that these effects are, at least in part, mediated by the binding of *CHAF1B* to the promoter region of ISGs, potentially competing with the binding of IFN α -activated transcription factors. This finding raises the possibility that during normal hematopoiesis, *CHAF1B* acts as a feedback mechanism to balance IFN responses, allowing proper proliferation and differentiation of hematopoietic cells. In agreement, knockdown of *Chaf1b* and *Chaf1a* was shown to increase the accessibility to chromatin at

specific enhancer sequences regulating differentiation of somatic cells in murine models (37). In another study, downregulation of these CAF-1 elements was shown to promote differentiation of myeloid stem and progenitor cells and the CAF-1 complex was found to control the access of ELFI transcription factor to specific DNA-binding sites regulating cell lineage identity (38). Notably, siRNA-mediated inhibition of *ULK1* expression, as well as inhibition of ULK1 kinase activity, increased the binding of CHAF1B to the promoter region of ISGs in the presence of IFN α treatment. Hence, ULK1 kinase activity in the presence of IFN α stimulation and ULK1 interaction with CHAF1B prevent binding of CHAF1B to these regions promoting transcription of ISGs. These results are consistent with our previous study in which we show that genetic-targeted inhibition and deletion of *ULK1* decreases IFN-induced transcription of ISGs (15). These results suggest that ULK1/CHAF1B levels and complex formation/disintegration might act as a tight mechanism to control IFN responses in MPN. In other studies, expression of CHAF1B protein was found to correlate with the proliferation marker Ki-67 in several solid tumors, including breast, prostate, endometrial, cervical, thyroid, renal, gastric, pancreatic, and colon cancers (39, 40). In addition, elevated CHAF1B expression has been associated with advanced tumor grade and staging in melanoma, high-grade glioma, salivary gland tumors, prostate, endometrial, renal, and cervical cancers (40–44). Future studies are required to investigate whether CHAF1B interacts with ULK1 in these solid tumors and to further elucidate the potential biological role of this complex in various tumor types. Specifically, assessing whether inhibition of ULK1 affects CHAF1B's protumorigenic role in other tumor types may exhibit important clinical significance. In our study, we identify CHAF1B as a novel negative regulator of IFN α -mediated transcription of ISGs and, consequently, of the antineoplastic effects in MPN. These results support the future development of small-molecule drug-targeted inhibitors, antisense oligonucleotides or degraders (e.g., proteolysis targeting chimeras [PROTACs]) of CHAF1B for the treatment of patients with MPN, as an approach to enhance IFN sensitivity and overcome IFN resistance.

Authors' Disclosures

L.C. Platanius reports grants from Northwestern during the conduct of the study. No disclosures were reported by the other authors.

References

- Ishii T, Bruno E, Hoffman R, Xu M. Involvement of various hematopoietic-cell lineages by the JAK2V617F mutation in polycythemia vera. *Blood* 2006;108:3128–34.
- Jamieson CH, Gotlib J, Durocher JA, Chao MP, Mariappan MR, Lay M, et al. The JAK2 V617F mutation occurs in hematopoietic stem cells in polycythemia vera and predisposes toward erythroid differentiation. *Proc Natl Acad Sci U S A* 2006;103:6224–29.
- McLornan D, Percy M, McMullin MF. JAK2 V617F: a single mutation in the myeloproliferative group of disorders. *Ulster Med J* 2006;75:112–9.
- Mead AJ, Mullally A. Myeloproliferative neoplasm stem cells. *Blood* 2017;129:1607–16.
- Grinfeld J, Nangalia J, Green AR. Molecular determinants of pathogenesis and clinical phenotype in myeloproliferative neoplasms. *Haematologica* 2017;102:7–17.
- Steensma DP. JAK2 V617F in myeloid disorders: molecular diagnostic techniques and their clinical utility: a paper from the 2005 William Beaumont Hospital Symposium on Molecular Pathology. *J Mol Diagn* 2006;8:397–411.
- Kiladjan JJ, Mesa RA, Hoffman R. The renaissance of interferon therapy for the treatment of myeloid malignancies. *Blood* 2011;117:4706–15.
- Vannucchi AM, Harrison CN. Emerging treatments for classical myeloproliferative neoplasms. *Blood* 2017;129:693–703.
- Quintás-Cardama A, Kantarjian H, Manshoury T, Luthra R, Estrov Z, Pierce S, et al. Pegylated interferon alfa-2a yields high rates of hematologic and molecular response in patients with advanced essential thrombocythemia and polycythemia vera. *J Clin Oncol* 2009;27:5418–24.
- Gisslinger H, Klade C, Georgiev P, Krochmalczyk D, Gercheva-Kyuchukova L, Egyed M, et al. Ropeginterferon alfa-2b versus standard therapy for polycythemia vera (PROUD-PV and CONTINUATION-PV): a randomised, non-inferiority, phase 3 trial and its extension study. *Lancet Haematol* 2020;7:e196–208.
- Wang BX, Fish EN. Global virus outbreaks: interferons as 1st responders. *Semin Immunol* 2019;43:101300.
- Platanius LC. Mechanisms of type-I- and type-II-interferon-mediated signaling. *Nat Rev Immunol* 2005;5:375–86.

Authors' Contributions

D. Saleiro: Conceptualization, formal analysis, investigation, methodology, writing-original draft. **E.M. Kosciuzuk:** Conceptualization, formal analysis, investigation, methodology, writing-original draft. **M. Fischietti:** Formal analysis, investigation, methodology, writing-review and editing. **R.E. Perez:** Investigation, methodology, writing-review and editing. **G.S. Yang:** Investigation, writing-review and editing. **F. Eckerdt:** Formal analysis, writing-review and editing. **E.M. Beauchamp:** Formal analysis, writing-review and editing. **Y. Hou:** Investigation, writing-review and editing. **Q. Wang:** Formal analysis, writing-review and editing. **R.S. Weinberg:** Resources, writing-review and editing. **E.N. Fish:** Formal analysis, writing-review and editing. **F. Yue:** Formal analysis, writing-review and editing. **R. Hoffman:** Resources, writing-review and editing. **L.C. Platanius:** Conceptualization, resources, supervision, funding acquisition, writing-original draft, project administration.

Acknowledgments

This work was supported by grants R01-CA77816 and R01-CA121192 from NCI, grant I01-CX000916 from the U.S. Department of Veterans Affairs, and a grant by the MPN Research Foundation, to L.C. Platanius. R.E. Perez was supported by grant T32-CA070085 from NCI. R. Hoffman and R.S. Weinberg are supported by PO1 CA108671 from NCI. G.S. Yang was supported by a grant from the Baker Program in Undergraduate Research, which is administered by Northwestern University's Weinberg College of Arts and Sciences. Proteomics services were performed by the Northwestern Proteomics Core Facility, generously supported by P30 CA060553 awarded to the Robert H. Lurie Comprehensive Cancer Center, instrumentation award (S10OD025194), and the National Resource for Translational and Developmental Proteomics supported by P41 GM108569.

Note

Supplementary data for this article are available at Cancer Research Communications Online (<https://aacrjournals.org/cancerrescommun/>).

Received January 04, 2023; revised March 28, 2023; accepted May 10, 2023; published first May 31, 2023.

13. Saleiro D, Plataniias LC. Interferon signaling in cancer. Non-canonical pathways and control of intracellular immune checkpoints. *Semin Immunol* 2019;43: 101299.
14. Mazewski C, Perez RE, Fish EN, Plataniias LC. Type I interferon (IFN)-regulated activation of canonical and non-canonical signaling pathways. *Front Immunol* 2020;11: 606456.
15. Saleiro D, Mehrotra S, Kroczyńska B, Beauchamp EM, Lisowski P, Majchrzak-Kita B, et al. Central role of ULK1 in type I interferon signaling. *Cell Rep* 2015;11: 605-17.
16. Saleiro D, Wen JQ, Kosciuczuk EM, Eckerdt F, Beauchamp EM, Oku CV, et al. Discovery of a signaling feedback circuit that defines interferon responses in myeloproliferative neoplasms. *Nat Commun* 2022;13: 1750.
17. Volk A, Crispino JD. The role of the chromatin assembly complex (CAF-1) and its p60 subunit (CHAF1B) in homeostasis and disease. *Biochim Biophys Acta* 2015;1849: 979-86.
18. Yacoub A, Mascarenhas J, Kosiorek H, Prchal JT, Berenson D, Baer MR, et al. Pegylated interferon alfa-2a for polycythemia vera or essential thrombocythemia resistant or intolerant to hydroxyurea. *Blood* 2019;134: 1498-509.
19. Saleiro D, Blyth GT, Kosciuczuk EM, Ozark PA, Majchrzak-Kita B, Arslan AD, et al. IFN- γ -inducible antiviral responses require ULK1-mediated activation of MLK3 and ERK5. *Sci Signal* 2018;11: eaap9921.
20. Zhou Y, Zhou B, Pache L, Chang M, Khodabakhshi AH, Tanaseichuk O, et al. Metascape provides a biologist-oriented resource for the analysis of systems-level datasets. *Nat Commun* 2019;10: 1523.
21. Rampal R, Al-Shahrour F, Abdel-Wahab O, Patel JP, Brunel JP, Mermel CH, et al. Integrated genomic analysis illustrates the central role of JAK-STAT pathway activation in myeloproliferative neoplasm pathogenesis. *Blood* 2014;123: e123-33.
22. Edgar R, Domrachev M, Lash AE. Gene Expression Omnibus: NCBI gene expression and hybridization array data repository. *Nucleic Acids Res* 2002;30: 207-10.
23. Fischietti M, Eckerdt F, Blyth GT, Mati WM, Oku CV, Perez RE, et al. Schlafen 5 as a novel therapeutic target in pancreatic ductal adenocarcinoma. *Oncogene* 2021;40: 3273-86.
24. Kosciuczuk EM, Mehrotra S, Saleiro D, Kroczyńska B, Majchrzak-Kita B, Lisowski P, et al. Sirtuin 2-mediated deacetylation of cyclin-dependent kinase 9 promotes STAT1 signaling in type I interferon responses. *J Biol Chem* 2019;294: 827-37.
25. Perez-Riverol Y, Bai J, Bandla C, García-Seisdedos D, Hewapathirana S, Kamatchinathan S, et al. The PRIDE database resources in 2022: a hub for mass spectrometry-based proteomics evidences. *Nucleic Acids Res* 2022;50: D543-52.
26. Joshi A, Iyengar R, Joo JH, Li-Harms XJ, Wright C, Marino R, et al. Nuclear ULK1 promotes cell death in response to oxidative stress through PARP1. *Cell Death Differ* 2016;23: 216-30.
27. Kraft C, Kijanska M, Kalie E, Siergiejuk E, Lee SS, Semplicio G, et al. Binding of the Atg1/ULK1 kinase to the ubiquitin-like protein Atg8 regulates autophagy. *EMBO J* 2012;31: 3691-703.
28. Volk A, Liang K, Suraneni P, Li X, Zhao J, Bulic M, et al. A CHAF1B-dependent molecular switch in hematopoiesis and leukemia pathogenesis. *Cancer Cell* 2018;34: 707-23.
29. Egan DF, Chun MG, Vamos M, Zou H, Rong J, Miller CJ, et al. Small molecule inhibition of the autophagy kinase ULK1 and identification of ULK1 substrates. *Mol Cell* 2015;59: 285-97.
30. Wang X, Rampal RK, Hu CS, Tripodi J, Farnoud N, Petersen B, et al. Characterization of disease-propagating stem cells responsible for myeloproliferative neoplasm-blast phase. *JCI Insight* 2022;7: e156534.
31. Moliterno AR, Ginzburg YZ, Hoffman R. Clinical insights into the origins of thrombosis in myeloproliferative neoplasms. *Blood* 2021;137: 1145-53.
32. Mascarenhas J, Kosiorek HE, Prchal JT, Rambaldi A, Berenson D, Yacoub A, et al. A randomized phase 3 trial of interferon- α vs hydroxyurea in polycythemia vera and essential thrombocythemia. *Blood* 2022;139: 2931-41.
33. Cheng L, Zhang X, Wang Y, Gan H, Xu X, Lv X, et al. Chromatin assembly factor 1 (CAF-1) facilitates the establishment of facultative heterochromatin during pluripotency exit. *Nucleic Acids Res* 2019;47: 11114-31.
34. Mattioli F, Gu Y, Yadav T, Balsbaugh JL, Harris MR, Findlay ES, et al. DNA-mediated association of two histone-bound complexes of yeast Chromatin Assembly Factor-1 (CAF-1) drives tetrasome assembly in the wake of DNA replication. *Elife* 2017;6: e22799.
35. Sykaras AG, Pergaris A, Theocharis S. Challenging accurate and feasible: CAF-1 as a tumour proliferation marker of diagnostic and prognostic value. *Cancers* 2021;13: 2575.
36. Saleiro D, Kosciuczuk EM, Plataniias LC. Beyond autophagy: new roles for ULK1 in immune signaling and interferon responses. *Cytokine Growth Factor Rev* 2016;29: 17-22.
37. Cheloufi S, Elling U, Hopfgartner B, Jung YL, Murn J, Ninova M, et al. The histone chaperone CAF-1 safeguards somatic cell identity. *Nature* 2015;528: 218-24.
38. Franklin R, Guo Y, He S, Chen M, Ji F, Zhou X, et al. Regulation of chromatin accessibility by the histone chaperone CAF-1 sustains lineage fidelity. *Nat Commun* 2022;13: 2350.
39. Polo SE, Theocharis SE, Klijanienko J, Savignoni A, Asselain B, Vielh P, et al. Chromatin assembly factor-1, a marker of clinical value to distinguish quiescent from proliferating cells. *Cancer Res* 2004;64: 2371-81.
40. Polo SE, Theocharis SE, Grandin L, Gambotti L, Antoni G, Savignoni A, et al. Clinical significance and prognostic value of chromatin assembly factor-1 overexpression in human solid tumours. *Histopathology* 2010;57: 716-24.
41. de Tayrac M, Aubry M, Saïkali S, Etcheverry A, Surlé C, Guénot F, et al. A 4-gene signature associated with clinical outcome in high-grade gliomas. *Clin Cancer Res* 2011;17: 317-27.
42. Mascolo M, Vecchione ML, Ilardi G, Scalvenzi M, Molea G, Di Benedetto M, et al. Overexpression of chromatin assembly factor-1/p60 helps to predict the prognosis of melanoma patients. *BMC Cancer* 2010;10: 63.
43. Staibano S, Mascolo M, Rocco A, Muzio LL, Ilardi G, Siano M, et al. The proliferation marker chromatin assembly factor-1 is of clinical value in predicting the biological behaviour of salivary gland tumours. *Oncol Rep* 2011;25: 13-22.
44. Staibano S, Mascolo M, Mancini FP, Kisslinger A, Salvatore G, Di Benedetto M, et al. Overexpression of chromatin assembly factor-1 (CAF-1) p60 is predictive of adverse behaviour of prostatic cancer. *Histopathology* 2009;54: 580-9.